

# 1-D, HOMOGENEOUS LIQUEFIED GAS SELF-PRESSURIZATION MODEL

*V.A. Zakirov, L. Li*  
Tsinghua University, Beijing, P.R. China

## Introduction

Liquefied gases have recently been employed instead of non-liquefied ones as propellants for small space vehicles [1-3] because:

- Their higher densities allow an increase in propellant loading for volume constrained spacecraft.
- Their self-pressurization feature eliminates a need in expulsion system.
- Often they can serve as multi-purpose propellants on spacecraft eliminating a need in the other propellants requiring separate storage hardware.

These advantages come along with shortcomings:

- Possible liquid sloshing in propellant storage tanks in-orbit.
- Possible two phase flows in thruster feed-lines.

- Possible loss of propellant self-pressurization feature due to its chilling during evaporation.

While the first two potential problems have their relatively simple solutions the last one requires special attention. This is because the loss of propellant's self-pressurization feature:

- leads to temporary liquefied gas propulsion system malfunction;
- is specific for each propellant storage system design.

Liquefied gas consumption out of storage tank during propulsion firings shifts liquid-to-vapor phase equilibrium inside causing liquid evaporation. Latent heat consumed in liquid-to-vapor phase change chills propellant inside the tank. This chilling causes vapor pressure drop. Vapor pressure drop reduces mass flow rate of propellant expelled out of the tank. These changes depend on heat rates flowing in and out of the system as well as heat and propellant mass stored by the system. Excessive initial propellant withdrawal out of the tank, therefore, chills liquefied gas fast causing sharp vapor pressure drop resulting in temporary fail-

ure of propellant feed to thruster(s). This will cause unexpected termination of thrusters' firing resulting in orbit maneuver failure.

To avoid propellant feed failure to thruster(s) excessive initial propellant consumption out of the tank must be prevented. Computer simulation of the liquefied gas evaporation process can help determining limiting value of propellant consumption to avoid the loss of liquefied gas self-pressurization feature, thus ensuring faultless operation.

### Model

The liquefied gas self-pressurization model is under development at Tsinghua Space Center. This model simulates thermodynamics of liquefied gas evaporation out of storage tank (see Fig. 1).

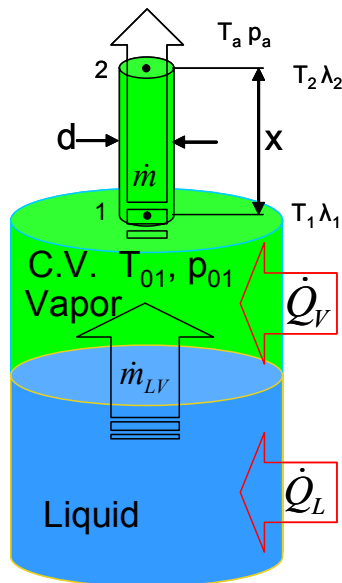


Fig. 1

In this model a liquefied gas inside storage tank has been selected as control volume (C.V.). In the beginning there is no flow of gas out of the tank so that the thermodynamic system is a closed one. A liquefied gas inside storage tank is assumed to remain at equilibrium for assigned temperature. Depending on initial conditions the equilibrium can be of single phase: vapor or liquid; or two-phase one: liquid-vapor.

Heat from the ambient is allowed to enter the control volume through tank walls and shift the equilibrium inside.

Once the tank is open the thermodynamic system changes to an open one. A liquefied gas leaves the tank through circular, constant cross-section area throat expelled by own vapor pressure. Depending on the heat rate entering the system through the tank walls and heat and mass stored in the system evaporation proceeds till new equilibrium state is reached inside.

### Assumptions

The following assumptions are made in this model:

1. Open/Closed system
2. Single component (liquefied gas)
3. Real gas
4. 1-Dimensional, homogeneous
5. Two-phase (liquid-vapor), or single-phase (gas (vapor), or liquid) equilibrium
6. Heat Capacity  $C_p=f(T)$  and enthalpy  $H=f(T)$  are functions of temperature
7. Regular geometry shape of storage tank (cylinder, sphere, and cylinder with spherical ends)
8. Heat transfer/adiabatic (optional) tank
9. Heat transfer/adiabatic (optional), frictional flow in the throat
10. Gravity (vertical)
11. No boiling
12. No chemical reactions
13. No mechanical work
14. No potential energy change

Since evaporation occurs on liquid-vapor interface which in the case of gravity, vertical tank position, and no boiling is minimal one the assessments made by the model are expected to be of conservative kind, i.e. represent the worst possible case. In-orbit, at zero-gravity condition liquid-vapor interface is expected to be more developed and larger so that evaporation

is expected to support higher expulsion flows than predicted.

### Equation System

Two main equations representing conservation of mass and energy inside control volume are the core of the model.

Mass balance for open system can be written as:

$$\frac{dm_{CV}}{dt} + \dot{m} = 0$$

where  $m_{CV}$  is mass of control volume, kg; while  $\dot{m}$  is liquefied gas mass flow rate leaving tank, kg/s;  $t$  is time, s.

Energy balance for open system can be written as:

$$\frac{dE_{CV}}{dt} = -\dot{m} \left( H_{Vout} + \frac{v^2}{2} \right) + \dot{Q}_{in}$$

where  $E_{CV}$  is energy of control volume, J;  $H_{Vout}$  – specific enthalpy (heat) of liquefied gas out of the tank, J/kg;  $v$  is velocity of liquefied gas out of the tank, m/s;  $\dot{Q}_{in}$  is a heat rate entering tank through walls, W.

Mass flow rate of liquefied gas out of the tank is determined as:

$$\dot{m} = \rho v A \quad (1)$$

where  $\rho$  – flow density, kg/m<sup>3</sup>;  $v$  – flow velocity, m/s;  $A$  – cross-sectional area of throat, m<sup>2</sup>.

Heat rate entering tank through walls:

$$\dot{Q}_{in} = h_L S_L (T_a - T) + h_V S_V (T_a - T)$$

where  $T_a$  and  $T$  are ambient and system temperatures respectively, K;  $h_L$  and  $h_V$  are liquid-ambient and vapor-ambient heat transfer coefficients, W/m<sup>2</sup>/K;  $S_L$  and  $S_V$  are contact surface areas between liquid and tank wall, and vapor and tank wall, m<sup>2</sup>.

The flow of gas out of the tank is approximated as flow through a constant diameter pipe with friction (see Fig. 1).

Two flow regimes are possible:

- sonic flow at the pipe's exit,  $\lambda_2 = 1$
- sub-sonic flow at the pipe's exit,  $\lambda_2 < 1$

where  $\lambda = v/v_s$  – dimensionless flow velocity;

while  $v_s = \sqrt{\gamma \frac{p}{\rho}}$  – sonic flow velocity, m/s.

Data required for calculation of gas properties have been taken from reference [0].

Liquefied gas heat capacity at constant pressure was calculated as:

$$C_p(T) = A + BT + CT^2 + DT^3 + ET^4, \text{ J/mol/K}$$

where  $A, B, C, D$  and  $E$  are coefficients given in [0];  $T$  – temperature, K.

Enthalpy of gas, J/mol:

$$H_V = H_f^0 + \int_{285.15K}^{T_0} C_p(T) dT$$

where  $H_f^0$  – standard enthalpy (heat) of formation for a gas, J/mol. [0]

Enthalpy of liquid, J/mol:

$$H_L = H_V - \Delta H_{vap}$$

where enthalpy of vaporization, kJ/mol:

$$\Delta H_{vap} = A \left( 1 - \frac{T}{T_c} \right)^n$$

and  $A$  and  $n$  are coefficients given in [0].

For saturated liquid and vapor mixture inside the tank:

$$m = m_L + m_V \quad \text{and} \quad V = V_L + V_V$$

total mass and volume are equal to sum of corresponding liquid and vapor quantities.

*Van der Waals* equation of state in reduced variables is used for calculation of gas properties for single phases:

$$P_r = \frac{8T_r}{3V_r - 1} - \frac{3}{V_r^2}$$

where  $p_r = \frac{p}{p_c}$ ,  $T_r = \frac{T}{T_c}$ , and  $V_r = \frac{V}{V_c}$ , while  $p_c$ ,  $V_c$ , and  $T_c$  – critical pressure, molar volume, and temperature, and,  $p$ ,  $V$ , and  $T$  – pressure, molar volume, and temperature of gas, respectively.

Liquid density is calculated as:

$$\rho_L = AB \left(1 - \frac{T}{T_c}\right)^n$$

where  $A$ ,  $B$ , and  $n$  are coefficients given in [0].

Gas density for saturated liquid-vapor region is obtained from liquid one using *Clapeyron's* equation:

$$\frac{dp}{dT} = \frac{\Delta H_{vap}}{T(V_{mV} - V_{mL})}$$

where  $\Delta H_{vap}$  – enthalpy (heat) of vaporization, J/mol;  $p$  – pressure, Pa;  $T$  – temperature, K;  $V_{mV} = \frac{\mu}{\rho}$  and  $V_{mL} = \frac{\mu}{\rho_L}$  – molar volumes for vapor and liquid respectively,

$m^3/mol$ ;  $\rho$  – vapor density,  $kg/m^3$ ;  $\mu$  – molar mass for gas,  $kg/mol$ .

Vapor pressure for liquefied gas as function of temperature:

$$\log_{10} p = A + \frac{B}{T} + C \log_{10} T + DT + ET^2$$

where  $A$ ,  $B$ ,  $C$ ,  $D$  and  $E$  are coefficients given in [0];  $p$  – pressure, mm of Hg;  $T$  – temperature, K.

### Results and Comparison

The computer model was used for simulation of nitrous oxide bleeding out of the tank. The experimental data were taken by the author during the test at the University of Surrey (U.K.) in 2001. This is the only relevant data available at Tsinghua Space Center at present.

Fig. 2 shows schematics and set-up for the nitrous oxide bleeding test. (The snapshot is taken at the end of the test when the gauge pressure in the tank dropped to about zero.) Before the test, a ~1 liter stainless steel tank was filled with liquid nitrous oxide. During the test, gaseous nitrous oxide bled out of the top of the tank. Nitrous oxide mass flow rate, liquid and vapor temperatures, and tank pressure were automatically recorded (see Fig. 3).

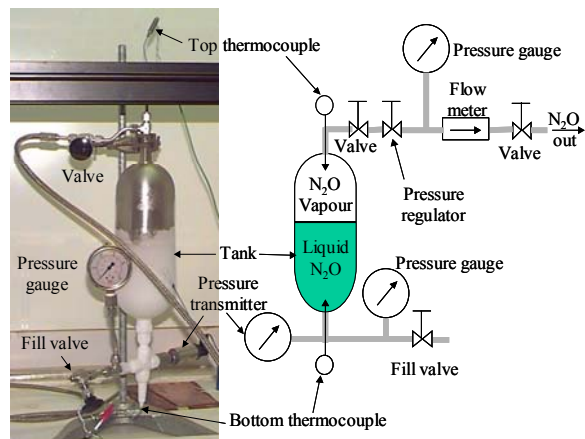


Fig. 2

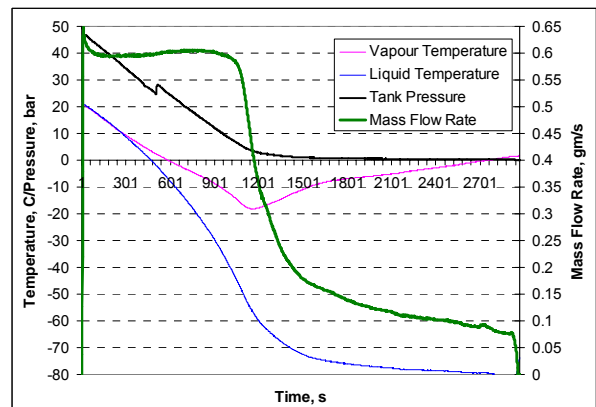


Fig. 3

The initial value (~0.65gm/s) was determined by the maximum nitrous oxide mass flow rate the flow-meter could support. Opening the valve was followed by slight drop in nitrous oxide mass flow rate that soon stabilized at about 0.6gm/s. While the mass flow rate remained somewhat constant for 16 minutes, the nitrous oxide vapor pressure and temperature both steadily decreased. After the tank's pressure dropped below 10bar, nitrous oxide mass

flow rate finally decreased. The increasing difference in liquid and vapor temperatures (that were originally the same) was due to the liquid's level drop upon nitrous oxide consumption. The spike on the pressure curve is due to the heat released by the phase change (enthalpy of fusion) when moisture condensed on the tank's wall froze.

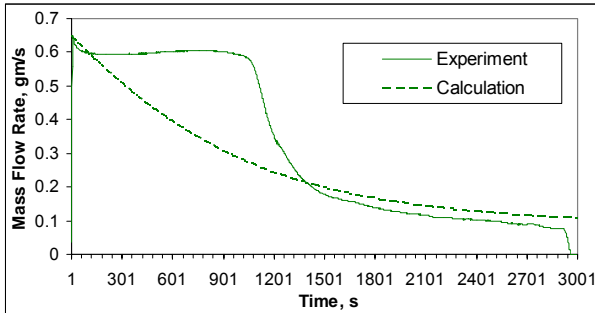


Fig. 4

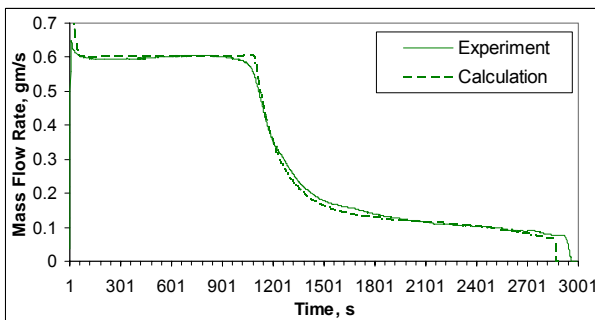


Fig. 5

Computer modeling of nitrous oxide evaporation process has revealed that the temperature of the tank's throat ( $T_{02}$ ) is critical for the gas mass flow rate out of storage tank.

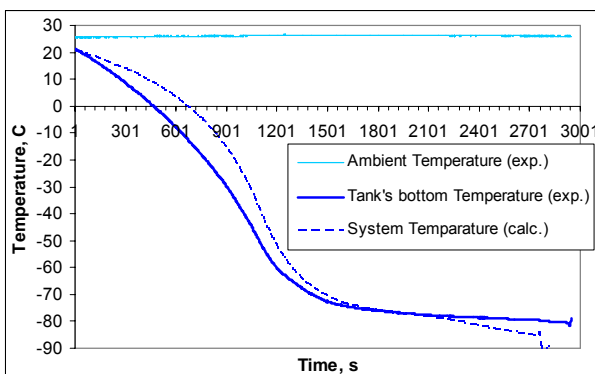


Fig. 6

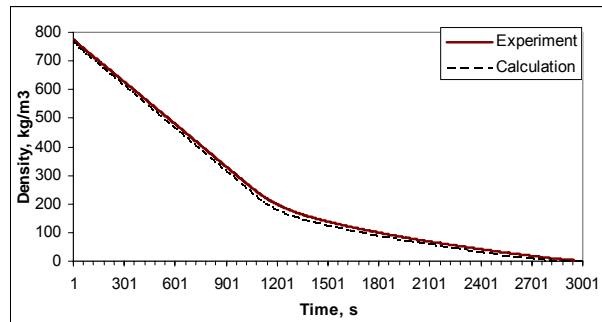


Fig. 7

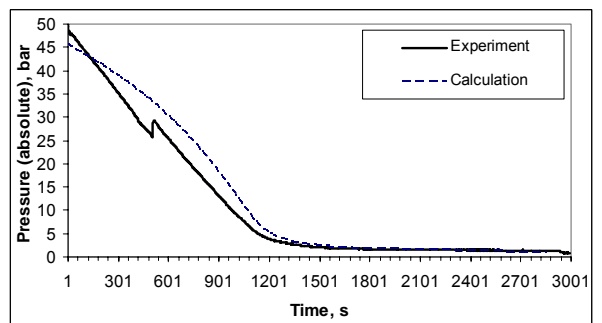


Fig. 8

In the case when the temperature of the throat is neglected, i.e. evaporation process is governed only by conditions inside the tank, the mass flow rate out of the tank drops continuously with time (see Fig. 4). During the experiment, however, the gas mass flow rate decreased with time as a step function.

After adjusting the throat temperature a good correlation between experimental and computational results has been achieved (see Fig. 5). This has demonstrated that the throat temperature during the test was "controlled" by some means. Revision of the experimental hardware revealed that the operation principle of *Omega* FMA5612-I series gas flow-meter used for nitrous oxide mass flow rate measurement employs gas flow heating [0]. The above conclusion has, therefore, been confirmed.

Taking an advantage of the experience gas flow heating can be employed to control mass flow rate during in-orbit liquefied gas expulsion. Such flow heating will also prevent liquid propagation downstream thruster feed-line.

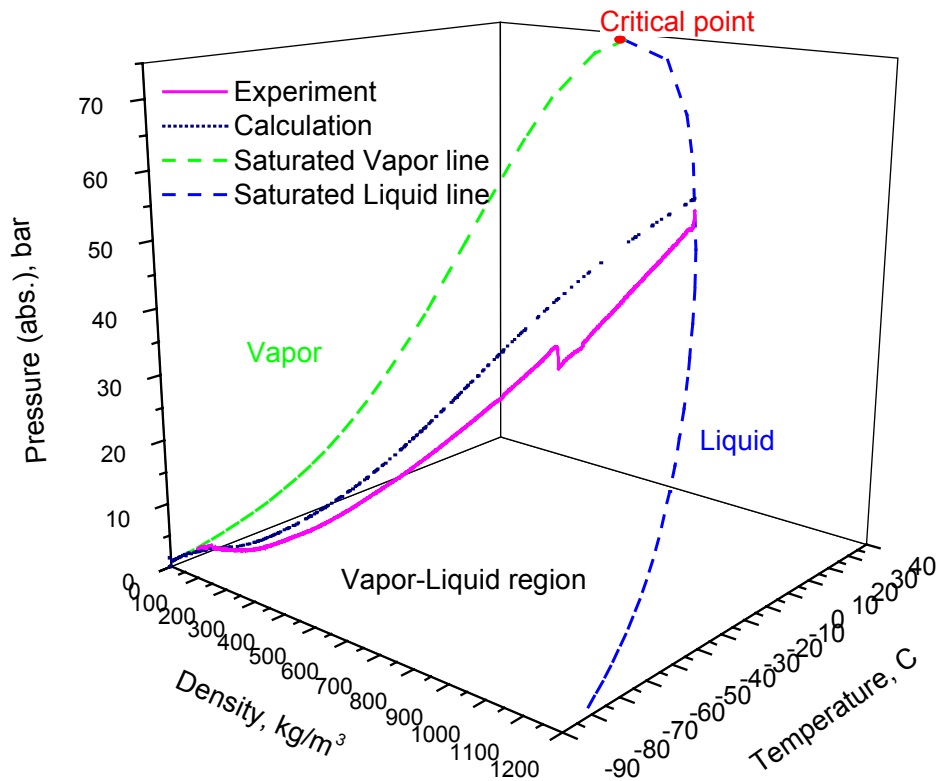


Fig. 9

Satisfactory fit to experimental data has also been demonstrated for temperature, density, and pressure calculated by the model (see Fig. 6 – Fig. 8).

Fig. 9 shows pressure-density-temperature plot of the process. The starting point representing tank fully loaded with nitrous oxide is located on saturated liquid line. After valve opening nitrous oxide flows out of the tank expelled by its own vapor pressure, causing pressure, density, and temperature drop inside. The process proceeds towards saturated vapor line till all liquid is evaporated and pressure of remained gas inside the tank reaches the ambient one. At that moment gas temperature drops almost to the boiling point of the liquefied gas.

Because evaporation occurs on liquid-vapor interface the process is sensitive to the interface temperature. Interface temperature

differs from average system temperature due to heat transfer. Since during the process liquid chills faster than vapor (see Fig. 3), and it has higher heat conductivity than vapor the interface temperature is closer to liquid one. In this case average system temperature is higher than the interface temperature so that higher temperatures and pressures are expected by the modeling. The discrepancy between experimental and calculation results (see Fig. 6, Fig. 8, and Fig. 9) confirms the expectation.

Modification of the model to 1-dimensional, heterogeneous one with average temperatures for liquid and vapor will improve the simulation accuracy since the interface temperature is expected to be closer to the average liquid than to system average temperature.

## Conclusions

One-dimensional, homogeneous model for liquefied gas self-pressurization has been developed at Tsinghua Space Center. The assumptions in this model are set to provide conservative assessments for expulsion mass flow rates that can be supported by a liquefied gas self-pressurization feature. This model has been successfully used for simulation of nitrous oxide evaporation out of storage tank. Comparison of calculated to experimental data revealed that during the test the liquefied gas evaporation out of storage tank was controlled through gas flow heating by in-line flow-meter. This experience is suggested for use during in-orbit operations. Satisfactory correlation between experimental and analytical results has been achieved, thus, it can be used for assessments of limiting value of propellant consumption out of the storage tank in-orbit to avoid the loss of liquefied gas self-pressurization feature.

The model accuracy can be further improved by its modification to 1-D, heterogeneous one.

## Future plans

The accuracy of the described model is expected to be improved by its modification

into 1-D, heterogeneous one. The suggested improvements are in process. Future experiments are planned for further model validation.

## References

- [1] Gibbon, D.M., J. Ward, and N. Kay, "The design, Development and Testing of a Propulsion System for the SNAP-1 Nanosatellite", SSC00-I-3, Proceedings of the 14th Annual AIAA/USU Conference on Small Satellites, the United States, 21-24 August 2000.
- [2] Wei Qing, The Research and Realization of Liquefied Gas Propulsion Technology, Proceedings of International Symposium on Space Propulsion 2004, Shanghai, P.R. of China, August 25-28, 2004.
- [3] Rachedi A., N. Hadj-Sahraoui, and A. Brewer, "AlSat-1: First Results of Multispectral Imager", Proceedings of XX<sup>th</sup> ISPRS Congress, Istanbul, Turkey, 12-23 July 2004.
- [4] Carl Yaws, *Matheson Gas Data Book*, 7<sup>th</sup> Edition, Matheson, 2001.
- [5] Omega Engineering Inc, An Omega Technologies Company, FMA5000 Series Electronic Mass Flowmeters. Operator's Manual, p.9; Internet: <http://www.omega.com/Manuals/manualpdf/M0698.pdf>